

# Estimation of Evapotranspiration Using Remote Sensing Data and Grid Computing: A Case Study in Dobrogea, Romania

CRISTINA SERBAN (GHERGINA), CARMEN MAFTEI & ALINA BARBULESCU

University "Ovidius" of Constanta

124 Mamaia Av.

ROMANIA

[cgherghina@gmail.com](mailto:cgherghina@gmail.com), [cmaftei@univ-ovidius.ro](mailto:cmaftei@univ-ovidius.ro), [alinadumitriu@yahoo.com](mailto:alinadumitriu@yahoo.com)

**Abstract:** - Estimating evapotranspiration is essential for understanding the water cycle of natural systems and for the management of the water resources in landscape systems. This paper presents a procedure to calculate the evapotranspiration using the remote sensing data and Grid Computing. Evapotranspiration was retrieved during satellite overpass and integrated for 24 hours on pixel-by-pixel base for daily estimation. As a result, a LST (Land Surface Temperature) and ET (Evapotranspiration) maps over the Dobrogea region were used for comparison with measured data provided by meteorological stations. The results are promising and appear to provide acceptable estimation over the study area.

**Key-Words:** - remote sensing, grid computing, evapotranspiration, land surface temperature

## 1 Introduction

Evapotranspiration (ET) represents the water loss by evaporation and plants transpiration [1]. The estimation of ET plays an essential role in all related activities to water resources management. In most studies (of hydrological research or design of hydro-technical systems) the determination from quantity point of views of water loss by evapotranspiration is representing the most important item of water balance. Unfortunately there are no experimental techniques well made to estimate the spatial distribution of the ET [21], even if the measurement gauges are allowing today an accurate estimation of the ET punctual.

A high number of methods were implemented in order to estimate ET for some particular weather conditions. These can be classified as follows (Singh VP et al. 1997): (i) water balance method which is based on the mass conservation principle applied to a given control volume (lysimeter, pan-evaporimeter, etc.), (ii) energy balance methods, (iii) empirical and semi-empirical methods (Thornthwaite 1938), (iv) aerodynamics methods, (v) combination methods (based on the original Penman (1948) method, this method combined two terms: the radiation term and the aerodynamic term). The analysis of those methods performances emphasized the need to formulate a "standard" evapotranspiration calculation. Therefore FAO Penman-Monteith [1] has been chosen as standard method for estimating ET. With all efforts made there are still remaining a series of issues which are making hard the estimation of ET: (i) ET values are valid for only one homogenous area related to the weather station

for which the estimations were made and in the weather conditions of that particular area, (ii) the need to have more weather data, (iii) in order to determine the spatial distribution of ET, it shall be known its values for several stations afterwards using miscellaneous methods of interpolation, (iv) knowing the type of vegetation and development stage of it as crop coefficient.

During the last three decades significant progresses were made in the determination of ET using remote sensing techniques. A study done by Courault [5] underlined a few methods which can be classified as follows: (i) empirical direct method – where the data coming out from satellite images processing are inserted as entry values in the empirical - semi/ empirical ET estimation models, (ii) residual methods of the energy budget which combining empirical methods with physical components (SEBAL, S-Sebi) and (iii) indirect methods (ISBA, Meso-NH). In the another study [13], the methods of ET estimation can be classified in two category: (i) (semi- empirical methods – which utilize empirical relationship and a minimum of meteorological data and (ii) analytical methods – involve the establishment of the physical process at the scale of interest.

Due to satellite images large size - up to 1 GB, Grid based architectures might be suitable platforms for their digital processing and analysis, because they offer the required computational power to process satellite data in real time [14]. The emergency of the Grid computation method offers two major advantages: (i) strong data-processing capability and (ii) the ability to use distributed computing resources to process the spatial data provided by a satellite image.

The objective of this paper is to develop a Grid computing application (a Computational Grid), which estimates the evapotranspiration at regional scale using the remote sensing data and a minimal amount of ground data.

## 2 Problem Formulation

The model used for ET estimation is based on the Triangle method. This method used the Priestly-Taylor equation modified by Jiang and Islam (2001), where the  $\alpha$  coefficient is a function of land surface temperature (LST) and Normalized Difference Vegetation Index (NDVI) [16].

The general formula of Priestly-Taylor equation is:

$$\lambda E = \alpha \cdot \left[ (R_n - G) \cdot \frac{\Delta}{\Delta + \gamma} \right], \quad (1)$$

where:  $\lambda E$  is the latent heat flux,  $\alpha$  is an empirical parameter,  $R_n$  is the net radiation (including long wave and short wave),  $G$  is the soil heat flux,  $\Delta$  is the slope of saturated vapor pressure and  $\gamma$  denotes psychometric constant.

The “beauty” of this equation is that all terms can be calculated using remotely sensed data. According with Jiang and Islam (2001) the parameter  $\alpha$  is obtained by two-step linear interpolation scheme: in the first step is obtained upper and lower bounds of  $\alpha$  for each specific NDVI class; NDVI classification is determined from the land use map. In our study, we consider four main land uses: water, urban, barren land and vegetation. We also consider a NDVI class for each NDVI value of the main land uses. The second step is to range the parameter  $\alpha$  within each NDVI class between the lowest temperature pixel and the highest temperature pixel. For this interpolation the relationship between LST and NDVI is used. Thus, the equation of the parameter  $\alpha$  is:

$$\alpha = \left( \frac{\Delta + \gamma}{\Delta} \right) \cdot \left( \frac{NDVI_i^{\max} - NDVI_i^{\min}}{NDVI_i^{\max}} \right) + \left( \frac{LST_i^{\max} - LST}{LST_i^{\max} - LST_i^{\min}} \right) \cdot \left( \frac{NDVI_i^{\min}}{NDVI_i^{\max}} \right) \quad (2)$$

where  $LST$  is value for current pixel,  $LST_i^{\max}$ ,  $LST_i^{\min}$ , and  $NDVI_i^{\max}$ ,  $NDVI_i^{\min}$  are the maximum and minimum values of surface temperature and NDVI, respectively, within NDVI class which has the current pixel.

Finally, the daily value of ET is:

$$\lambda E_{daily} = \left[ \left( \frac{NDVI_i^{\max} - NDVI_i^{\min}}{NDVI_i^{\max}} \right) \cdot \left( \frac{LST_i^{\max} - LST}{LST_i^{\max} - LST_i^{\min}} \right) + \left( \frac{NDVI_i^{\min}}{NDVI_i^{\max}} \right) \cdot \frac{2DL \cdot (R_i - G_i)}{\pi \cdot \sin(\pi \cdot t/DL)} \right] \quad (3)$$

where: DL is total day length, hours, and  $t$  is time beginning at sunrise. To obtain the 24 hours totals, the daily ET values are multiplied by 1.1 for all days.

To compute the LST we implemented the Jimenez-Munoz and Sobrino's algorithm [20] which needs a single ground data (the total atmospheric water vapor content –  $w$ ). In order to calculate the LST firstly we compute the NDVI:

$$NDVI = \frac{band4 - band3}{band4 + band3} \quad (4)$$

and the Land Surface Emissivity (LSE), based on NDVI values [20]:

$$LSE = 1.0094 + 0.047 * \ln(NDVI) \quad (5)$$

When the NDVI value is out of the range (0.157–0.727), the corresponding input LSE constant values are used [18].

Now, we can calculate LST

$$LST = \gamma[LSE^{-1} \cdot (\psi_1 L_{sensor} + \psi_2) + \psi_3] + \delta \quad (6)$$

$$\text{with } \gamma = \left\{ \frac{c^2 L_{sensor}}{T_{sensor}^2} \left[ \frac{\lambda^4}{c_1} L_{sensor} + \lambda^{-1} \right] \right\}^{-1} \quad (7)$$

and

$$\delta = -\gamma L_{sensor} + T_{sensor}, \quad (8)$$

where:

$L_{sensor}$  = gain \* DN + bias - spectral radiance

DN - the digital number of a pixel,

$$T_{sensor} = \frac{K_2}{\ln(K_1 / L_{sensor} + 1)} - \text{brightness temperature}$$

$\lambda$  - the effective wavelength,

$$c_1 = 1.19104 * 10^8 W \mu m^4 m^{-2} sr^{-1}, c^2 = 14387.7 \mu m K,$$

$\psi_i, i = \overline{1,3}$  - atmospheric parameters, which are functions of the total atmospheric water vapor content ( $w$ )

### 2.1 Study area

Dobrogea area has been chosen for this study due to its importance in the Romanian economy. Dobrogea together with Romanian plain and South of Moldova are among the driest areas, where the crops cannot grow without irrigation systems. It is absolutely necessary to know ET as management method of the water sources for irrigation for the design and exploitation of the irrigation systems.

#### 2.1.1 Dobrogea area

Dobrogea is a region situated in the South – East of Romania, between the Black Sea and the lower Danube River (Fig.1).

Dobrogea (without the Danube Delta) is a plateau with hilly aspect. Generally, Dobrogea's climate is temperate-continental. The air temperature average is slightly over 11°C towards the littoral area and the

Danube floodplain, and no more than 10-11°C in the North and center [15].

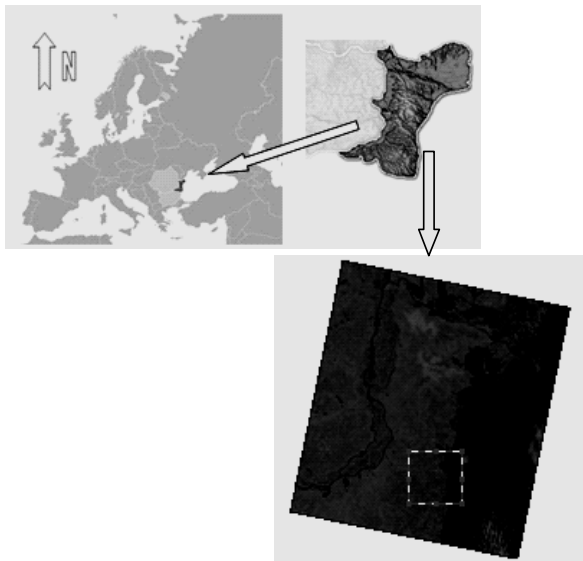


Fig.1. Dobrogea area and Landsat ETM+ “false color” image; bands combination: 742

### 2.1.2 Satellite Data

In this study, we used one subset of Landsat ETM+ image dated 7<sup>th</sup> June 2000 that covers the Dobrogea area corresponding to Constanta weather station. The image is in geo-tiff format and was downloaded from Landsat Imagery, [9]. A radiometric calibration (atmospheric corrections) was the pre-processing step that was taken. The bands ETM+ 3 and 4 were analyzed with respect to the NDVI values, the band ETM+ 6 was used to compute the LST values, and the other bands (ETM+ 1, 2, 5 and 7) were processed to estimate the albedo values.

### 2.1.3 Meteorological Data

In addition to satellite data, this study needed two ground meteorological data: the total atmospheric water vapor content -  $w$ , used in LST estimation algorithm, and the air temperature -  $T_{air}$ . These parameters were obtained from the weather station of Constanta, located on the study area.

## 3 Problem Solution

### 3.1. Satellite Data Pre-processing

Satellite data pre-processing comprise of radiometric calibrations (atmospheric corrections) for ETM+ bands 3 and 4. These bands are used to retrieve NDVI (Normalized Difference Vegetation Index) values on which the LST (land Surface Temperature) estimation algorithm is based on. It is possible to obtain NDVI values from at-sensor or TOA (Top of Atmospheric)

reflectivities, called as NDVI<sub>TOA</sub>, but it is more accurate to atmospherically correct the TOA values in order to obtain at-surface reflectivities and, in this way, estimate NDVI values more representative of the natural surfaces, called as NDVI<sub>surf</sub>.

In this study we applied an atmospheric correction based on image data, developed by [3], its main advantage being that the data necessary in order to carry out the atmospheric correction are obtained from the image itself. The at-surface reflectivity is calculated with the following equation:

$$\rho_{surf} = \frac{\pi(L_{sensor} - L_p)d^2}{E_0 \cos \theta_z T_z}, \quad (9)$$

where  $L_{sensor}$  is at-sensor radiance,  $T_z$  is the atmospheric transmissivity between the sun and the surface ( $T_z \approx \cos \theta_z$  [4]),  $\theta_z$  is the zenithal solar angle,  $E_0$  is the spectral solar irradiance on the top of the atmosphere [2],  $d$  is the Earth-Sun distance [2], and  $L_p$  is the radiance resulted from the interaction of the electromagnetic radiance with the atmospheric components (molecules and aerosols) that can be obtained according to:

$$L_p = L_{min} - L_{1\%}, \quad (10)$$

where  $L_{min}$  is the radiance that corresponds to a digital count value for which the sum of all the pixels with digital counts lower or equal to this value is equal to the 0.01% of all the pixels from the image considered.  $L_{min}$  was calculated through DOS (Dark Object Subtraction) technique [4], while the term  $L_{1\%}$  is given by

$$L_{1\%} = \frac{0.01 \cos \theta_z T_z E_0}{\pi d^2}, \quad (11)$$

### 3.2. Approach

Our application meets the requirements of a virtual organization (VO) member which access to a local database of large satellite images and wants to apply several satellite image processing operations in order to estimate the daily evapotranspiration. The operations to be performed are implemented in special client's codes and are to be run on the Computational Grid.

Due to the large size of a satellite image, the full image transfer should be avoided. Therefore, a satellite image will be split into a number of sub-images equal with the number of workstations of the Grid Cluster. The image processing algorithms will also be split into independent tasks that can be performed in parallel and that are requiring similar computing effort.

The following components are needed: (i) at the user's node: the satellite bands, the client's codes and some minimal facilities to access Grid infrastructure; (ii) at remote computing nodes: the Grid middleware which allows the execution of client's codes.

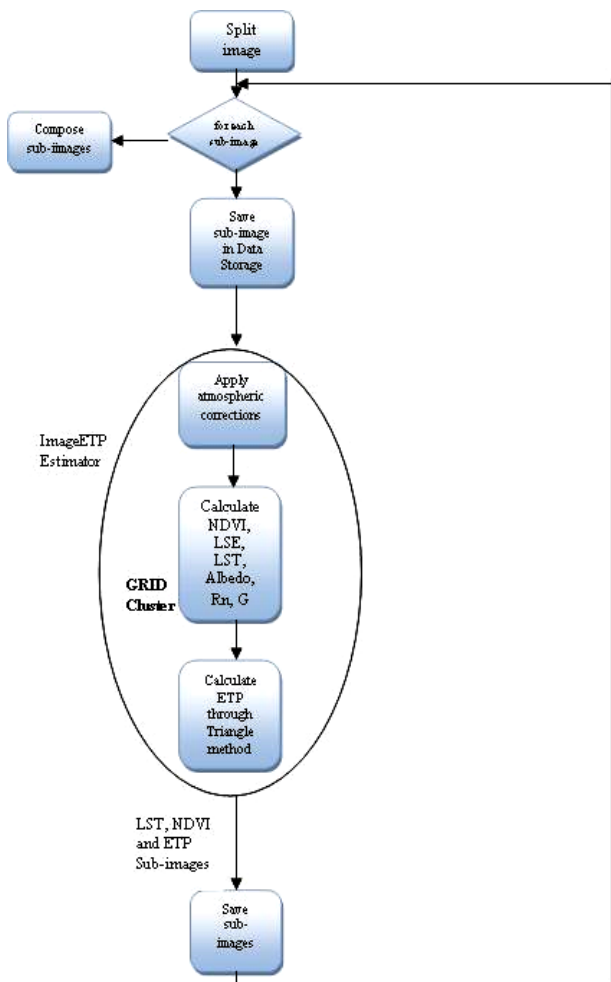


Fig.2. The logical processing steps for each sub-image

The client's code consists of three components (Fig.2): (i) the Splitter that takes a satellite image and split it into a number of sub-images; (ii) the Image ET Estimator, that receives a sub-image, applies the processing algorithms and produces the output files (LST image, ET image and 3 text files of NDVI, LST and ET float values); (iii) the Composer that merges the resulting sub-images.

The Splitter and the Composer programs run only at the user's site where the large satellite images are residing. The Image ET Estimator and the sub-images are submitted for processing on the Computational Grid.

The user uploads the image files and submits the jobs to the Grid. After the successful finish of the jobs, the user can download the resulting images.

The service works as follows (Fig. 3): (i) the user uploads the image files using Grid FTP and submits the job to the Grid; (ii) the image file(s) are transferred to code site; (iii) the Splitter code is called and the smaller pieces of image(s) are produced as well as the files needed by PBS to launch the Image ETP Estimator operation on each sub-image; (iv) The Job Manager of Globus Toolkit 4 take over the files and interpret them

and finally PBS sends the jobs on the cluster of workstations.

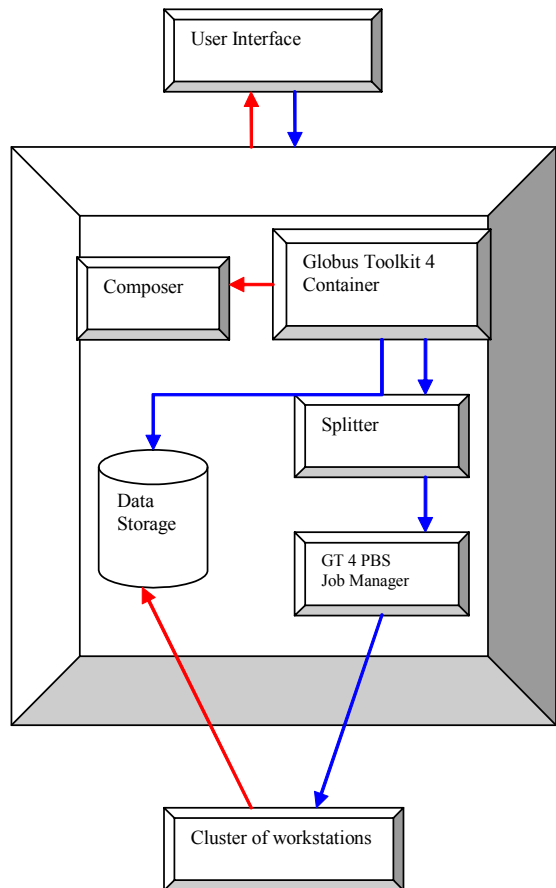


Fig.3. The components of the service and their interactions

After the job executions the output files are stored on the code site. The user can access the output files through the user interface. The client's code were written in Java and tested on the Computational Grid provided by Globus Toolkit 4.

Also, a Web-based client interface (Fig.4), for a service that launches the codes has been built using JSP, Tomcat/5.5 and MySQL.

The user interface is a web form titled 'ETP estimator'. It features a 'New' button, a 'Submit' button, and a 'Reset' button. Below the buttons is a section for 'ETP estimator' with fields for 'Band 1' through 'Band 7', each with a 'Browse' button. A 'Status' section contains a large empty text area.

Fig.4. The user interface

The testing environment contains 2 PC nodes (Intel P4, 2.4 GHz, 1GB DDRAM) connected at 100 Mbps

and allows processing images of size up to 10 MB. The tests that we performed proved that the presented application is efficient in terms of computation time and easy to use (Table 1). The application output data consist of the files described in Table 2.

Table 1. Response time for the sub-images processing

No. of nodes	Response time (s)	File Size
1	8.641	3000 x 3000
2	2.831	750 x 750

Table 2. The output data

File (type)	Description
.txt	Text file with LST values (°C)
.txt	Text file with NDVI values
.txt	Text file with daily ET values
.txt	Text file with statistical data for each NDVI class (min, max, mean, stdev for NDVI, LST and ET values)
.tiff	LST Map
.tiff	ET Map

The LST Map (Fig.5) shows that the LST values for the study area vary between 22°C la 48°C, which is consistent with the ground meteorological data measured by Constanta weather station (measurements are taken at intervals of 6 hours) (Table 3 and Fig.6).



Fig.5. LST Image - Dobrogea region, 2000

The temperature difference between the actual mean soil surface temperature at the time when satellite passed and the remote sensed mean land surface temperature ( $0.73^{\circ}\text{C}$ ) is considered acceptable.

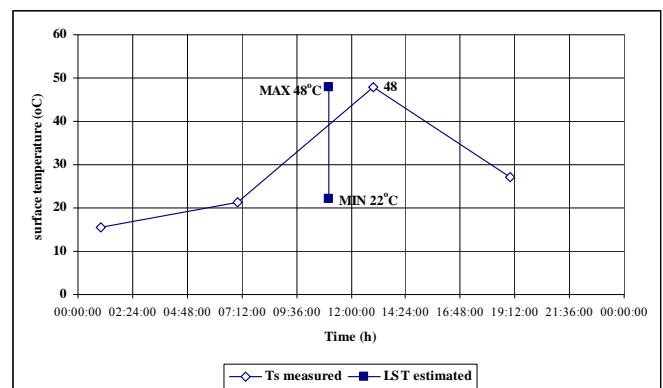


Fig.6. LST values measured and estimated

Table 3. Comparison between actual mean LST and remote sensed mean LST

Date:	June 7, 2000
Satellite Overpass Time	
GMT	8.32
Local Time	11.32
Weather Station Data	
Air Temp (°C)	23.3
Humidity (%)	82
Total atmospheric water vapor content (g/cm <sup>3</sup> )	2.3
Mean LST (°C)	
At 7 am:	21.2
At 13 am:	48
At 11:30 am:	42.31
Remote sensed LST	
Mean LST (°C)	41.58

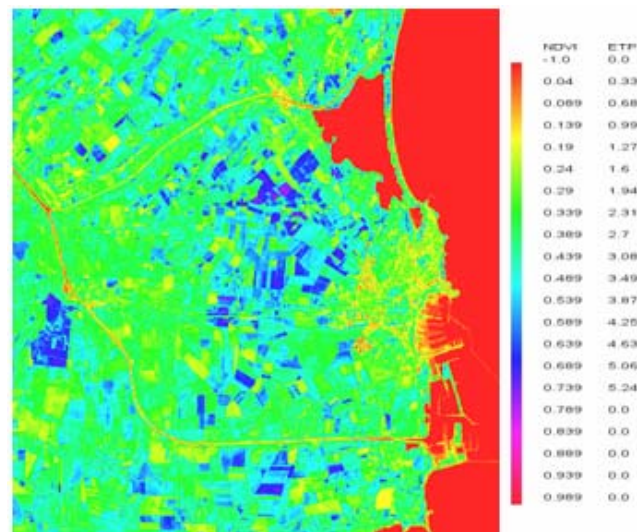


Fig.7. ETP Image - Dobrogea region, 2000

Regarding the values of the evapotranspiration (ET), the results are shown in Fig. 7. Evapotranspiration ranges between 0.33 and 5.24mm/day. According to Constanta weather station, the multi-annual average of the evapotranspiration in June is between 4.5 and 5.6 mm/day, so the estimation error is eligible.

## 4 Conclusion

In this paper we present a Computational Grid to estimate the daily ET values in Dobrogea region using remote sensing imagery. The application is meant to be used by those who want to do such studies but don't have the computational resources they need. We implemented an ET estimation algorithm, the Triangle method, which is based on the modified Priestly-Taylor equation and whose inputs are mainly satellite data. The proposed approach is applied to Constanta area to estimate ET in 7<sup>th</sup> June 2010. The results are promising and show that the method utilized can derive reasonable estimates for surface temperature (LST) and evapotranspiration (ET).

A Web-based client interface was also built. We consider the application will be useful and convenient for those who use satellite remote sensing to study the geographical distribution of evapotranspiration, and consequently water demand in large cultivated areas for irrigation purposes and sustainable water resources management, and have typical workstations, with no special computing and storing resources for computationally intensive satellite image processing and no license for a commercial image processing tool.

**Acknowledgments.** This article was supported by CNCSIS – UEFISCSU, project number PNII – IDEI 262/2007.

### References:

- [1] Allen, G. R., Pereira, L. S., Raes, D. and Smith, M. *Crop Evapotranspiration-Guidelines for computing crop water requirements* FAO Irrigation and Drainage Paper 56. FAO, Rome, Italy, 1998
- [2] Chander, G., Markham, B L., Helder, D.L., Summary of current radiometric calibration coefficients for Landsat MSS, TM, ETM+, and EO-1 ALI sensors, *Remote Sensing of Environment* 113 (2009) 893–903, 2009
- [3] Chavez P.S., An improved dark-object subtraction technique for atmospheric scattering correction of multispectral data, *Remote Sensing of Environment*, 24:459-479, 1988
- [4] Chavez, S., Image-based atmospheric correction—revisited and Improved, *Photogrammetric Engineering and Remote Sensing*, 62(9), 1996, pp. 1025– 1036,
- [5] Courault, D., Seguin, B., Olioso, A., Review to estimate evapotranspiration from remote sensing data: some examples from the simplified relationship to the use of mesoscale atmospheric models. In *ICID workshop on remote sensing of ET for large regions*, Montpellier, France, 2003, pp. 1 – 17
- [6] Digital Image Processing Tutorial, <http://www.accusoft.com/resourcecenter/tutorials/>
- [7] ENVI Tutorial, [www.itvis.com/Envi/docs/tutorials/Classification Methods.pdf](http://www.itvis.com/Envi/docs/tutorials/Classification%20Methods.pdf)
- [8] Jacob, B., Brown, M., Fukui, K., Trivedi, N., *Introduction to Grid Computing*, SG24-6778-00 2005, <http://ibm.com/redbooks>,
- [9] Jiang, L. and Islam, S. Estimation of surface evaporation map over southern Great Plains using remote sensing data, *Water Resour. Res.*, Vol. 37(2), 2001, pp.329-340,
- [10] Jinqu Zhang, Yunpeng Wang, Yan Li, A C++ program for retrieving land surface temperature from the data of Landsat TM/ETM+ band6, *Computers & Geosciences* 32 2006, pp. 1796–1805
- [11] Keiser, K., Ramachandran, R., Rushing, J., Conover, H., Graves, S., *Distributed Services Technology for Earth Science Data Processing*
- [12] Landsat Imagery, <http://www.landsat.org/ortho/index.php>
- [13] Li Zhao Liang, et al., A Review of Current Methodologies for Regional Sensed Data, *Sensor Data*, 9, 2009, pp. 3801-3853
- [14] Li Sheng-yang, Zhu Chong-guang, GE Ping-ju, Remote Sensing Image Deblurring, Based on Grid Computation, *J. China Univ. of Mining & Tech. (English Edition)*, Vol. 16(4), 2006, pp. 409-412.
- [15] Maftei, C., Bărbulescu, A., 2008, Statistical analysis of climate evolution in Dobrudja region, *Lecture Notes in Engineering and Computer sciences*, WCE, vol.II, 2008, pp. 1082 -1087
- [16] Nourbaeva, G., Kazama, S., Sawamoto, M., Assement of Daily Evapotranspiration Using Remote Sensing Data, Environmental Informatics Archives, Vol 1, 2003, pp. 421-427
- [17] Petcu, D. *Arhitecturi si tehnologii Grid*, Editura Eubaea, 2006
- [18] Petcu, D., Iordan, V., *Grid Service based on GIMP for Processing Remote Sensing Images*, Procs. SYNASC 2006, Timisoara, Los Alamitos (ISBN 07695 2740 X), pp.251-258, 2006
- [19] Remote Sensing Guide, <http://cbc.rs-gis.amnh.org/>
- [20] Sobrino J., Jiménez-unoz J.C., Paolini L., Land surface temperature retrieval from LANDSAT TM 5, *Remote Sensing of Environment* 90, 2004, pp. 434 – 440
- [21] Wallace, J.S. Calculating evaporation: resistance to factors *Agricultural and Forest Meteorology* Vol. 73(3-4), 1995, pp 353 – 366
- [22] Wu. J., Wang. D., Bauer, M.E.. Image-based atmospheric correction of QuickBird imagery of Minnesota cropland, *Remote Sensing of Environment*, 99, 2005, pp. 315 – 325